

12

NAMRL 1308

SPECIFIC ABSORPTION RATE IN A SITTING RHESUS MODEL  
AT 225, 1290, AND 5950 MHZ FOR E, H, AND K POLARIZATIONS

Toby A. Griner and Richard G. Olsen

AD-A145 435



DTIC  
SELECTED  
SEP 13 1984  
E

23 April 1984

NAVY AEROSPACE MEDICAL RESEARCH LABORATORY  
PENSACOLA, FLORIDA

Approved for public release; distribution unlimited.

84 09 05 020

DTIC FILE COPY

Approved for public release; distribution unlimited.

SPECIFIC ABSORPTION RATE IN A SITTING RHESUS MODEL  
AT 225, 1290, AND 5950 MHz FOR E, H, AND K POLARIZATIONS

Toby A. Griner and Richard G. Olsen

Naval Medical Research and Development Command  
MF58.524.02C-0004

Reviewed by

Ashton Graybiel, M.D.  
Chief Scientific Advisor

Approved and Released by

Captain W. M. Houk, MC, USN  
Commanding Officer

23 April 1984

NAVAL AEROSPACE MEDICAL RESEARCH LABORATORY  
NAVAL AIR STATION  
PENSACOLA, FLORIDA 32508

## SUMMARY PAGE

### THE PROBLEM

Previous radio-frequency dosimetry studies of the E-polarized sitting rhesus model have shown higher specific absorption rates (SAR) than predicted by theoretical estimates based on a prolate spheroidal model. It was postulated that partial-body resonances tended to enhance the whole-body absorption. The purpose of this study was to further investigate the effects of enhanced whole-body SARs for three primary orthogonal orientations at three widely spaced irradiation frequencies.

### FINDINGS

Enhanced whole-body SARs have been found at both the E and H polarizations in the decade of frequencies above resonance. At a frequency nearly 30 times above resonance, no enhanced SAR was observed, and the results agreed well with predictions from theoretical models. The enhanced SARs are attributed to resonances in the limbs and to postural orientations that allow strong coupling to the incident fields.

### RECOMMENDATIONS

It is recommended that the parameters responsible for the enhanced H-polarized SAR be studied more closely since the disparity between our results and theoretical predictions was the largest for H polarization. It could be possible that other body postures could enhance the H field coupling even more.

### ACKNOWLEDGEMENT

The authors wish to acknowledge the valuable assistance of Mr. John F. Forstall who participated in many phases of this study.

Accession For	
NTIS GRA&I	<input checked="checked" type="checkbox"/>
DTIC TAB	<input type="checkbox"/>
Unannounced	<input type="checkbox"/>
Justification	
By	
Distribution/	
Availability Codes	
Dist	Avail and/or Special
A-1	



## INTRODUCTION

Radio-frequency (RF) dosimetry of animals and man has been approached by both theoretical and experimental methods to quantify electromagnetic (EM) absorption characteristics. Theoretical methods, based on prolate spheroids and ellipsoids, were used in the radio-frequency radiation dosimetry handbooks (1, 2, 5), and these handbooks have been useful to predict whole-body specific absorption rates (SAR). Using block models of man, Gandhi *et al* (3) predicted partial-body and multibody effects which would alter the whole-body absorption in the post resonance region. Experimental dosimetry, using figurines (4) or full-size models (6-9) of tissue-equivalent materials, has been used to determine whole-body and partial-body SAR and to characterize the distribution of RF absorption.

Quantitative dosimetric analysis of a tissue-equivalent primate model has been conducted in this laboratory to derive realistic estimates of the whole-body SAR and the RF absorption distribution for use in experiments with primate subjects, and to provide a basis for extrapolation to man. These studies have been restricted to a fixed-posture sitting rhesus model to provide a coherent basis for comparison. Although some measurements have used temperature probes to examine depth penetration, or thermographic scans to study the surface absorption distribution, the primary method of measurement has been calorimetric. This method provides good repeatability, avoids extrapolation from point measurements, and is useful for both whole-body and partial-body SAR measurements.

In past studies at this laboratory, partial-body and multibody (adjacent limbs) resonances were observed to significantly contribute to EM absorption in the E-polarized rhesus model at 1290 MHz (7, 8). When compared with handbook predictions, whole-body SAR was enhanced by 50 per cent and the primary contribution was from the legs. Later studies of the E-polarized rhesus model at 225 MHz (9), a frequency near whole-body resonance, showed good agreement with handbook predictions although partial-body measurements found elevated SAR in the arms of the model.

In the present study, whole-body absorption of the rhesus model has been continued at 225 MHz, 1290 MHz, and 5950 MHz for three orthogonal polarizations (E, H, and K). For reference purposes, our measurements are compared with handbook predictions for a one-year-old child whose prolate spheroid model best approximates the rhesus model.

Our results for the three polarizations were in good agreement with handbook predictions at 5950 MHz. At 1290 MHz and 225 MHz, however, our results show increased absorption at the H polarization. The increased SAR is attributed to contributions from the limbs which couple strongly to the incident fields for certain postures, frequencies, and orientations.

## MATERIALS AND METHODS

These experiments were similar in design to previous studies of the sitting rhesus model (7-9). The model (Figure 1) had a mass of 8.8 kg, a sitting height of 73 cm, and was enclosed in a polyurethane mold (Eccofoam FP, Emerson and Cummings). In an attempt to prevent moisture penetration,

the mold was first coated with plastic (Plastidip Int. Type PDS) and then painted with a coat of lacquer. This model was about one kilogram lower in mass than the original model used in previous studies.



Figure 1

Photograph of the sitting rhesus model. The front half of the mold has been removed.

The frequency range of our studies required three different microwave anechoic chambers. The 225-MHz chamber and generating equipment has been previously described (9). This chamber uses a copper-lined plywood horn in a commercial anechoic chamber (Technical Bulletin No. 31-2, Emerson and Cummings), and the model was placed at .74 times the minimum far-field distance. The 1290-MHz chamber was also described previously (7, 8). RF energy was provided by an AN/FPS-8 military radar set operating with a pulse width of 3  $\mu$ s and a repetition rate of 330 pps. The model was placed in the far field at a distance of 200 cm from a horn irradiator. The 5950-MHz irradiation system used a microwave generator (Singer, Model 6600) with a continuous wave (CW) signal amplified to 700 watts by a klystron amplifier (Model 11106B, MCL, Inc.). Waveguide connected the amplifier to a standard gain horn (Model 642 Narda, Inc.), and the power level was monitored with a power meter (General Microwave Model 471) fed from a crossguide coupler. The 5950-MHz anechoic chamber has been described (6). A wall of absorber was inserted as a backstop behind the rhesus model at a distance of 400 cm from the antenna.

Whole-body energy absorption of the model was measured with a gradient-layer calorimeter (Model SEC-A-3601, Thermonics, Inc.) as previously described (8). Measurements of the calorimeter output, room temperature, and waterbath temperature were monitored with a desktop computer data acquisition system (HP Model 3052A) throughout the cooling period and for one hour prior to the measurement. When the model had stabilized after exposure (usually about 16 hours), initial temperature, final temperature, mass, irradiation time, and other parameters were entered on the keyboard. The desktop computer processed the stored data, and reported the rate of energy absorption in watts. In all SAR determinations, three replicate measurements were made using fresh batches of tissue-equivalent material. The replicate measurements were averaged, and SAR (normalized to 1 mW/cm<sup>2</sup>) was calculated using the average power density and the average mass of the three replications. The incident power density was determined by measuring eight model locations in the chamber (in the absence of the model) with a Model 8306B radiation monitor (Narda).

Since our results were to be compared with the handbook predictions, the one-year-old child model was chosen for comparison, and the predictions were taken from the second edition handbook curves. The one-year-old child prolate spheroid model, with a height of 74 cm and a width of 16 cm, was most similar to the rhesus model. The rhesus model has a height of 73 cm and abdomen width of 13 cm (The relative sizes of the models are shown in Figure 2). The rhesus model, however, has a mass of approximately 8.8 kgm compared to a 10-kg mass for the child model. Figure 2 also gives the dimensions of major body parts in terms of the free-space wavelength of each irradiation frequency.

The three orthogonal polarizations of the model used in this study are consistent with normal definitions. Since the model is not axially symmetrical, the orientation chosen was the model facing the antenna, head up, with the long axis of the body either parallel to the E field (E polarization) or to the H field (H polarization). In the K polarization, the model was irradiated from the head to toe with the thighs of the model parallel to

the E-field vector. The thighs project outward from the model and were exposed to a field density about 25 per cent less than the tip of the head.

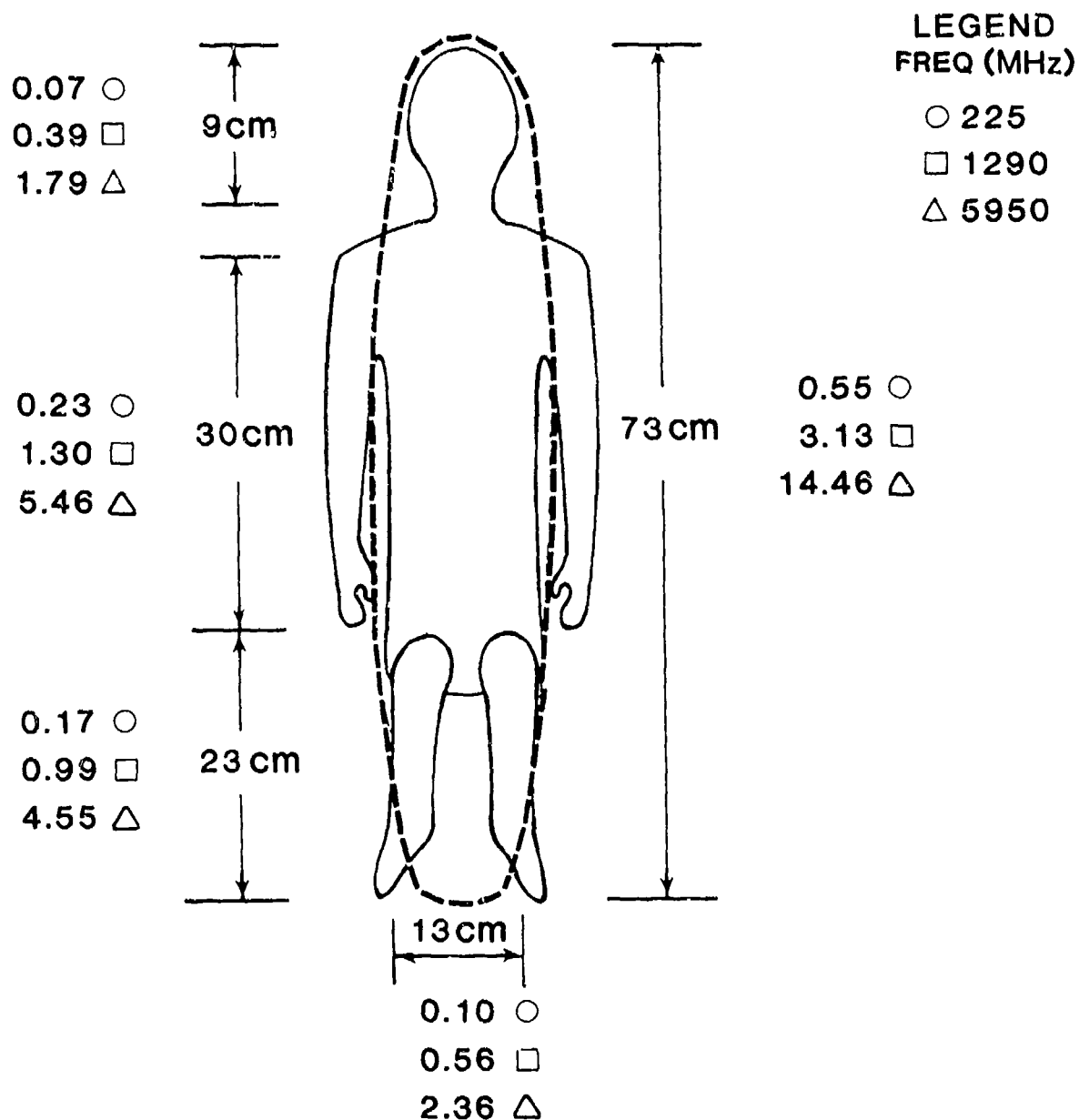


Figure 2

Comparison of the rhesus model and the prolate spheroid model (dashed line). Limb lengths and their length to wavelength ratio are shown for 225, 1290, and 5950 MHz.

To study the surface distribution of the absorbed energy in these models, a thermographic imager (UTI-Spectrotherm) was used to measure the temperature of the front surface of the model after a 20-minute exposure. The thermograms were recorded on film after the resolution and baseline adjustments were made to insure that the coldest and warmest areas were within the unsaturated range of the thermographic imager. These thermograms provided relative, qualitative measurement of the distribution in front surface absorption.

## RESULTS

Figures 3-5 give graphic comparisons of our whole-body SAR results to those predicted for the prolate spheroidal model. The data are summarized in Table I. The greatest disparity between predicted and experimental SAR was in the H polarization. It is expected that the K-polarization results would be closer together if the revised theoretical curve for K polarization were available from the third edition handbook for the one-year-old child.

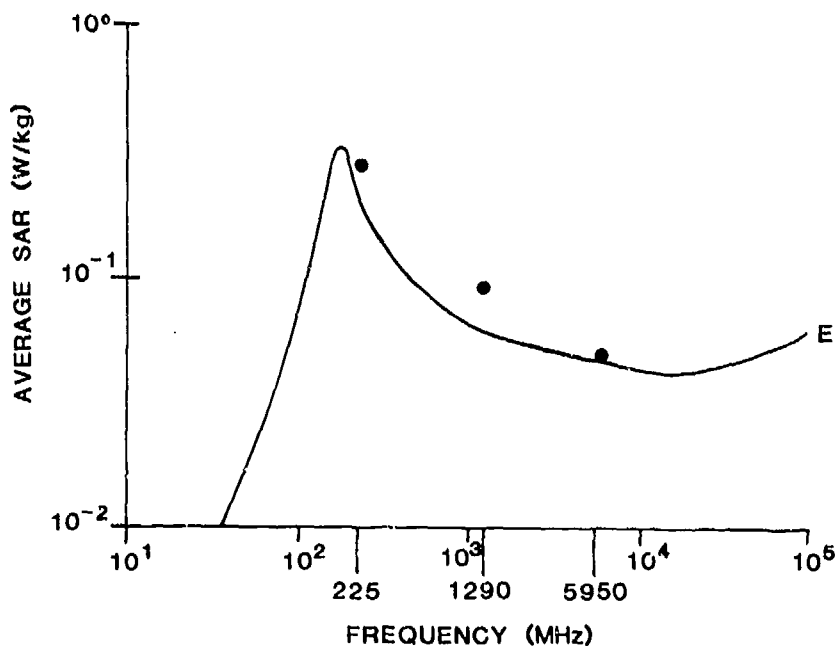


Figure 3

Comparison of the E-polarized rhesus model whole-body SAR measurement (circles) with the theoretical model (solid). SAR is normalized to 1.0 mW/cm<sup>2</sup>.

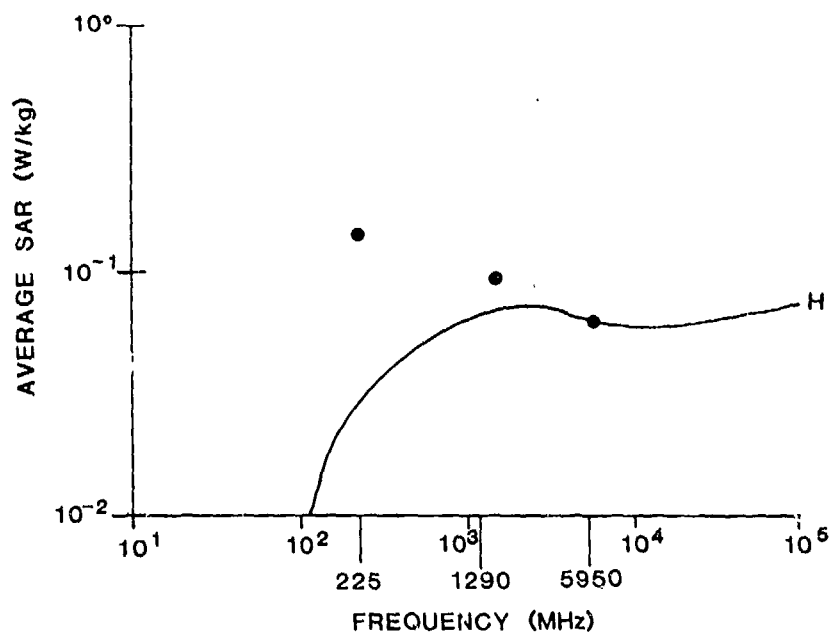


Figure 4

Comparison of the H-polarized rhesus model whole-body SAR measurement (circles) with the theoretical model (solid). SAR is normalized to  $1.0 \text{ mW/cm}^2$ .

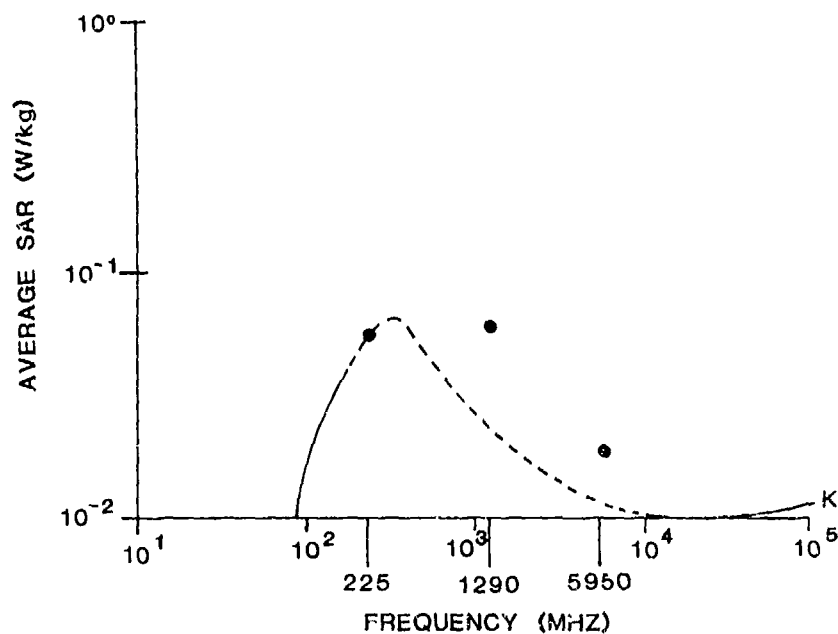


Figure 5

Comparison of the K-polarized rhesus model whole-body SAR measurement (circles) with the theoretical model (solid). Dashed line is estimated. SAR is normalized to  $1.0 \text{ mW/cm}^2$ .

Our results show enhanced SAR for both the E and H polarizations at 1290 MHz and the enhancement was by about 40 per cent. At the H polarization for 225 MHz, the whole-body SAR was enhanced by 100 per cent. At 5950 MHz, our results for the E and H polarization showed good agreement.

TABLE I

Summary of the Rhesus Model Whole-Body SAR Measurements

$((W/kg)/(mW/cm^2) \pm SD)$

Polarization	225 MHz	1290 MHz	5950 MHz
E	0.28 $\pm$ .025	.089 $\pm$ .004	0.053 $\pm$ .006
H	0.14 $\pm$ .001	.093 $\pm$ .002	0.064 $\pm$ .008
K	0.059 $\pm$ .013	.066 $\pm$ .005	0.020 $\pm$ .003

The thermographic imaging results are shown in Figures 6 and 7 in which warmer areas are depicted in lighter tones. Figure 6 is a typical preirradiation thermogram. For 225 MHz, the E-polarization thermogram shows the highest SAR in the arms (previously measured by calorimetry methods to be .92 Wkg/mW/cm<sup>2</sup>, about 5 times the SAR of the torso). For the H polarization, the thermograms show a higher SAR in the groin region. The K polarization thermograms show an unexpected warm region in the legs.

For 1290 MHz, the arms and legs are the warmer regions. The legs were previously measured to be 8 times that of the torso and the arms to be 4 times that of the torso. For the H polarization, an absorption distribution similar to that observed for the H-polarized 225-MHz model can be seen, although the thermographic measurements indicate that this heating is less than that of the 225-MHz measurement. For the K polarization, leg heating can be seen, but appears to be less than at 225 MHz.

At 5950 MHz, the distribution is more uniform over the body for both E and H polarizations. The knee area appears warmer in the K polarization.



Figure 6  
Preirradiation thermogram of the rhesus model.

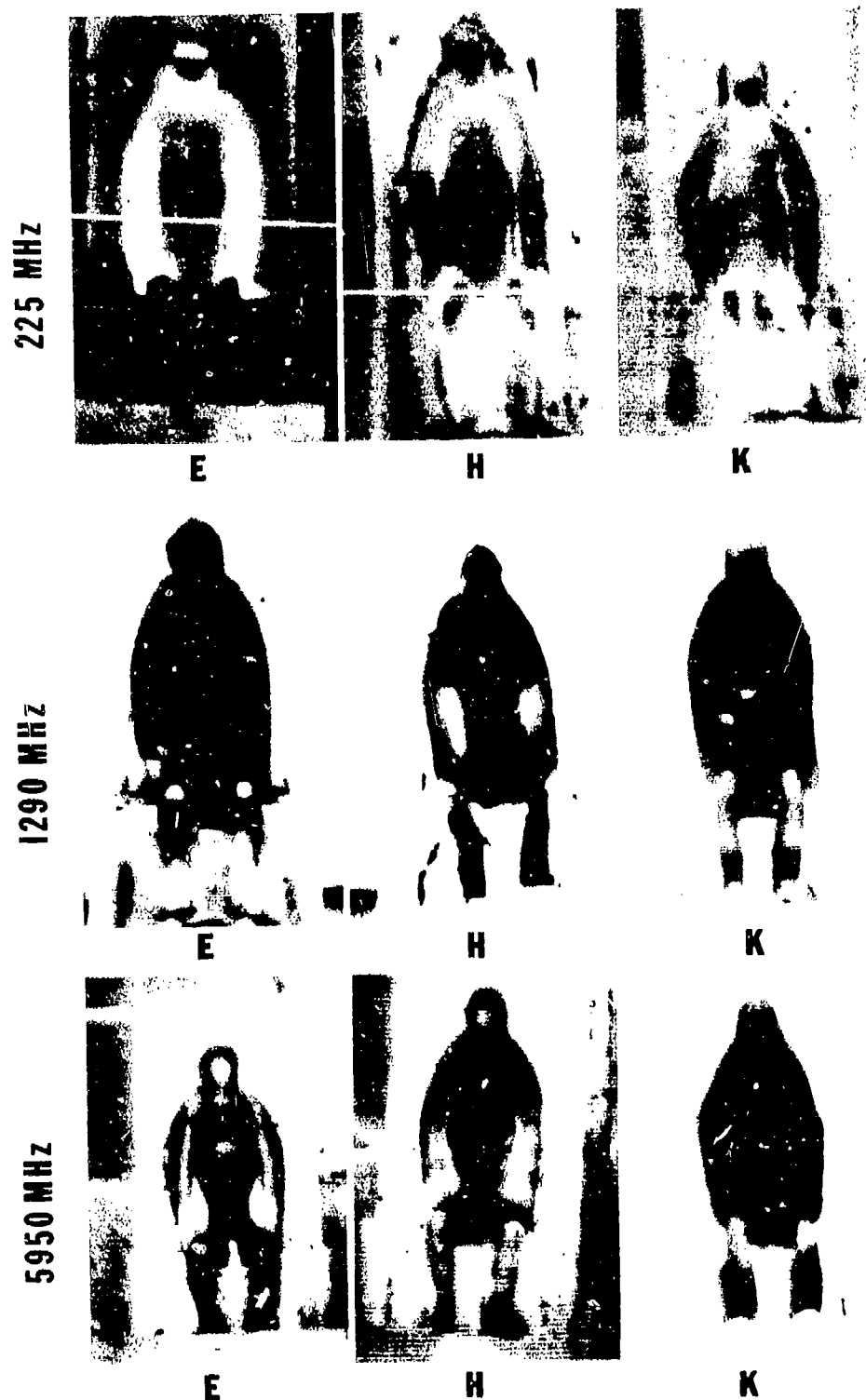


Figure 7

Thermograms of the rhesus model for 225, 1290, and 5950 MHz.

## DISCUSSION

When compared to handbook predictions, our results of the whole-body SAR measurements of the rhesus model show significantly higher RF absorption at 1290 MHz for both E and H polarizations. The distribution of absorption has shown relatively high SAR in the arms, and, in particular, the legs for the E polarization. The distribution for the H polarizations exhibited an entirely different heating pattern in which the groin, and, to some extent, the area between the arms and torso showed elevated SARs. These localized heating areas appear at the intersection of limbs rather than in the limbs themselves. The enhancement in whole-body SAR for both the E and H polarization was about the same and may indicate that an H-polarization resonance phenomena is responsible for the elevated whole-body SAR observed. Partial-body measurements in the H-polarized models, however, have not been made to quantify the SAR.

At 225 MHz, the E-polarized whole-body SAR was elevated by about 10 per cent, but the enhancement is not considered significant. The H polarization at 225 MHz, which has a distribution similar to that at 1290 MHz, shows enhanced SAR in the groin and arm-torso regions. The whole-body SAR was elevated by 100 per cent and the higher absorption indicated by the thermogram in the groin may be the explanation. If this high SAR in the groin region is due to a resonance phenomena, then the wavelength ratios of the limbs at 225 MHz appear to be closer to H resonance than those wavelength ratios at 1290 MHz.

At 5950 MHz, the whole-body SAR comparisons show good agreement and indicate that partial-body resonances do not enhance the whole-body SAR.

For the K-polarization measurements, the thermograms have shown leg or leg-knee heating regardless of frequency although the more intense heating is found at the lower frequency. Since the lower leg portion of the model was K polarized and was farthest from the antenna, it was not expected that this portion would exhibit higher SARs. The thermogram results, however, clearly show lower leg heating which would be expected to enhance the whole-body SAR. The thighs of the model, which were aligned with the E field, were expected to be resonate at 1290 MHz since the wavelength ratios are close to one wavelength. However, a thigh heating pattern is not clearly shown in the thermograms. The 225-MHz results agree well with theoretical predictions, in spite of the higher absorption in the lower legs, but comparisons for K polarization at 1290 and 5950 MHz are inconclusive until revised theoretical calculations are available.

Previous studies of the partial-body SAR rates at E polarization have shown a strong correlation with resonant limbs. At 1290 MHz, the largest contribution was from the legs with a SAR of  $0.24 \text{ (W/kg)/(mW/cm}^2\text{)}$ , and with a wavelength ratio of 1.0 for the length and 0.56 for the distance between the legs. The arms, with a ratio of 1.3, showed a SAR of 0.5 as compared to a torso SAR of 0.03. The resulting whole-body SAR of 0.1 would indicate that these resonant parts significantly increased the whole-body SAR. At a frequency near whole-body resonance (225 MHz), partial-body measurements have shown the largest SAR (.92) in the arms, whose wavelength ratio of .23 is closest to one-half wavelength. The results of this study

at 5950 MHz do not reveal enhanced SAR and indicate that the limbs were not resonant, as would be expected since all ratios were greater than 1.8. However, a consistent result from partial-body measurements indicate that limbs closest to one-half wave were the largest contributors to whole-body SAR; however, limbs from .2 to 1.5 wavelengths also contributed to the whole-body SAR, particularly, if both arms and legs were within this range. Given the range of limb sizes in this model, a large portion of the post-resonant frequency range could exhibit enhanced SAR resulting from various contributions from the limbs.

### CONCLUSIONS

Whole-body RF absorption was significantly above theoretical predictions in a full-size muscle-equivalent rhesus model in a frequency region where partial-body resonance occurred. For the E-polarized model, these elevated SARs were correlated with resonant limbs that exhibited much higher energy absorption than the torso. An apparent resonance phenomena in the H-polarized model was observed that also elevated the whole-body SAR, but exhibited a different distribution of absorbed energy than did the E-polarized model.

These studies show that higher-than-predicted SARs can occur in realistic models whose limbs or limb-body configurations exhibit resonance that couples strongly to the incident fields. Enhanced SARs can be expected for those frequencies near resonance or in the post resonance region where limb dimensions approach one-half wavelength. These results suggest that whole-body SAR is strongly influenced by the limb position and body posture and can be much higher than predicted for spheroidal models.

## REFERENCES

1. Durney, C.H., Johnson, C.C., Massoudi, H., Iskander, M.F., Lords, J.L., Reyser, D.K., Allen, S.J., and Mitchell, J.C., Radio frequency radiation handbook (second edition), report SAR-TR-78-22 USAF School of Aviation Medicine, Aerospace Medical Division (AFSC), Brooks Air Force Base, Tx, 1978.
2. Durney, C.H., Iskander, M.F., Massoudi, H., Stewart, J.A., and Mitchell, J.C., Radiofrequency Radiation Dosimetry Handbook (Third Edition), Report SAM-TR-80-32 USAF School of Aviation Medicine, Aerospace Medical Division (AFSC) Brooks AFB, TX, 1980.
3. Gandhi, O.P., Hagmann, M.F., and D'Andrea, J.A., Part-body and Multibody effects on absorption of radio frequency electromagnetic energy by animals and by models of man. Radio Science 14(6S): 15-21, 1979.
4. Guy, A.W., Webb, M.D., and Sorenson, C.C., Determinations of power absorption in man exposed to high frequency electromagnetic fields by thermographic measurements in scale models. IEEE Trans. Biomed. Eng. BME-23: 361-371, 1976.
5. Johnson, C.C., Durney, C.H., Barber, T.W., Massoudi, H., Allen, S.J., and Mitchell, J.C., Radio frequency dosimetry handbook, Report SAM-TR-76-35 USAF School of Aviation Medicine, Aerospace Medical Division (AFSC) Brooks AFB, TX, 1976.
6. Olsen, R.G., Preliminary studies: Far-field microwave dosimetric measurements of a full-scale model of man. Journal of Microwave Power, 14(4): 383-388, 1979.
7. Olsen, R.G., Griner, T.A., and Prettyman, G.D., Far-field microwave dosimetry in a rhesus monkey model. Bioelectromagnetics 1: 149-160, 1980.
8. Olsen, R.G. and Griner, T.A., Partial-body absorption resonances in a sitting rhesus model at 1.29 GHz, Radiation and Environmental Biophysics 21: 33-43, 1982.
9. Olsen, R.G. and Griner, T.A., Electromagnetic dosimetry in a sitting rhesus model at 225 MHz. Bioelectromagnetics 3: 385-389, 1982.

UNCLASSIFIED

SECURITY CLASSIFICATION OF THIS PAGE (When Data Entered)

REPORT DOCUMENTATION PAGE		READ INSTRUCTIONS BEFORE COMPLETING FORM
1. REPORT NUMBER NAMRL- 1308	2. GOVT ACCESSION NO. AD-A145 435	3. RECIPIENT'S CATALOG NUMBER
4. TITLE (and Subtitle) Specific Absorption Rate in a Sitting Rhesus Model at 225, 1290, and 5950 MHz for E, H, and K Polarizations		5. TYPE OF REPORT & PERIOD COVERED Interim
7. AUTHOR(s) Toby A. Griner and Richard G. Olsen		6. PERFORMING ORG. REPORT NUMBER
9. PERFORMING ORGANIZATION NAME AND ADDRESS Naval Aerospace Medical Research Laboratory Naval Air Station Pensacola, Florida 32508		10. PROGRAM ELEMENT, PROJECT, TASK AREA & WORK UNIT NUMBERS MF58.524.02C-0004 L211582
11. CONTROLLING OFFICE NAME AND ADDRESS Naval Medical Research & Development Command Naval Medical Command, National Capital Region Bethesda, Maryland		12. REPORT DATE 23 April 1984
14. MONITORING AGENCY NAME & ADDRESS (if different from Controlling Office)		13. NUMBER OF PAGES 14
		15. SECURITY CLASS. (of this report) UNCLASSIFIED
		15a. DECLASSIFICATION/DOWNGRADING SCHEDULE
16. DISTRIBUTION STATEMENT (of this Report) Approved for public release; distribution unlimited		
17. DISTRIBUTION STATEMENT (of the abstract entered in Block 20, if different from Report)		
18. SUPPLEMENTARY NOTES		
19. KEY WORDS (Continue on reverse side if necessary and identify by block number) Dosimetry, Specific Absorption Rate, Polarization, Rhesus model, Radio-Frequency, Calorimetry, Thermographic		
20. ABSTRACT (Continue on reverse side if necessary and identify by block number) To extend our knowledge in radio-frequency (RF) and microwave dosimetry, average whole-body specific absorption rate (SAR) and front surface temperature measurements in a sitting rhesus model were obtained for three orthogonal orientations of irradiation at a frequency near whole-body resonance (225 MHz), at a frequency of previously observed partial-body resonances (1290 MHz), and at a frequency nearly 30 times above resonance (5950 MHz). An 8.8 kg model, composed of muscle-equivalent material, was irradiated in anechoic chambers. Whole-body absorbed RF energy was measured with a		

DD FORM 1 JAN 73 1473

EDITION OF 1 NOV 65 IS OBSOLETE

S N 0102-LF-014-6601

UNCLASSIFIED

SECURITY CLASSIFICATION OF THIS PAGE (When Data Entered)

UNCLASSIFIED

SECURITY CLASSIFICATION OF THIS PAGE (When Data Entered)

gradient-layer calorimeter, and the front surface temperature distribution was measured thermographically. Compared with published theoretical data based on a prolate spheroidal model of nearly equal weight and height, significantly elevated SARs were found for the E and H polarizations at 1290 MHz and for the H polarization at 225 MHz, but good agreement was observed for the other configurations. The disparity was attributed to partial-body resonances in the limbs or to postural orientations which coupled strongly to the incident magnetic field. It is concluded that theoretical methods in dosimetry are least applicable in the decade of frequencies above resonance where the arms, legs, and head may exhibit resonant absorption.

S/N 0102- LF- 014- 6601

UNCLASSIFIED

SECURITY CLASSIFICATION OF THIS PAGE (When Data Entered)